

MIT Open Access Articles

Quantum Dot Targeting with Lipoic Acid Ligase and HaloTag for Single-Molecule Imaging on Living Cells

The MIT Faculty has made this article openly available. **Please share** how this access benefits you. Your story matters.

Citation: Liu, Daniel S., William S. Phipps, Ken H. Loh, Mark Howarth, and Alice Y. Ting. "Quantum Dot Targeting with Lipoic Acid Ligase and HaloTag for Single-Molecule Imaging on Living Cells." ACS Nano (December 5, 2012): 11080-11087.

As Published: <http://dx.doi.org/10.1021/nn304793z>

Publisher: American Chemical Society (ACS)

Persistent URL: <http://hdl.handle.net/1721.1/95744>

Version: Author's final manuscript: final author's manuscript post peer review, without publisher's formatting or copy editing

Terms of use: Creative Commons Attribution-Noncommercial-Share Alike





Published in final edited form as:

ACS Nano. 2012 December 21; 6(12): 11080–11087. doi:10.1021/nn304793z.

Quantum Dot Targeting with Lipoic Acid Ligase and HaloTag for Single Molecule Imaging on Living Cells

Daniel S. Liu, William S. Phipps, Ken H. Loh, Mark Howarth[§], and Alice Y. Ting^{*}

Department of Chemistry, Massachusetts Institute of Technology, 77 Massachusetts Avenue, Room 18-496, Cambridge, MA 02139, USA

Abstract

We present a methodology for targeting quantum dots to proteins on living cells in two steps. In the first step, *E. coli* lipoic acid ligase (LplA) site-specifically attaches 10-bromodecanoic acid onto a 13-amino acid peptide that can be genetically fused to a protein of interest. In the second step, quantum dots derivatized with HaloTag, a modified haloalkane dehalogenase, react with the ligated bromodecanoic acid to form a covalent adduct. We found this targeting method to be specific, fast, and fully orthogonal to a previously reported and analogous quantum dot targeting method using *E. coli* biotin ligase and streptavidin. We used these two methods in combination for two-color quantum dot visualization of different proteins expressed on the same cell or on neighboring cells. Both methods were also used to track single molecules of neurexin, a synaptic adhesion protein, to measure its lateral diffusion in the presence of neuroligin, its trans-synaptic adhesion partner.

Keywords

Quantum dot targeting; fluorescence microscopy; single molecule imaging; lipoic acid ligase; HaloTag

Quantum dots (QDs) are extremely bright and photostable fluorescent nanoparticles that can be detected with very high sensitivity, down to the single molecule level, in complex biological environments such as living cells.¹ To visualize specific proteins, QDs are typically conjugated to antibodies that in turn recognize specific cellular proteins. Because this is limited, however, by the low affinity and/or specificity of many antibodies, and the lack of antibodies to recognize extracellular portions of many proteins of interest, our lab previously developed an alternative QD targeting method based on biotin ligase and streptavidin. In this method, proteins of interest are genetically fused to an extracellular 15-amino acid tag called the “acceptor peptide” (AP). The AP sequence is site-specifically biotinylated by *E. coli* biotin ligase (BirA), then labeled with streptavidin-conjugated QDs.² QD targeting by BirA has been used for single molecule imaging of numerous cellular proteins.^{3–5}

There is great interest in multicolor imaging of cellular proteins, and therefore we wished to develop a second, orthogonal QD targeting method. With such a method it would be

^{*}Corresponding ating@mit.edu.

[§]Present address: Department of Biochemistry, University of Oxford, South Parks Road, Oxford, OX1 3QU, United Kingdom

ASSOCIATED CONTENT

Supporting Information available: plasmid cloning; synthesis and characterization of haloalkane substrates; LplA enzyme and protein substrate purification; conjugation of HaloTag to Alexa Fluor dyes; Supporting Figures and associated methods. This material is available free of charge *via* the Internet at <http://pubs.acs.org>.

possible to image two different proteins in the same cell, or in neighboring cells, each with single molecule sensitivity. Additionally, although the biotin-streptavidin binding affinity is very high, the off-rate increases 10-fold or more when each is conjugated to a macromolecule, leading to dissociation on the order of hours,^{6,7} or on the order of seconds with applied force.^{8,9} We were therefore also motivated to develop a covalent targeting method for long-term imaging applications. We recognized that a second labeling system analogous to BirA/biotin/streptavidin would also have applications apart from QD targeting. For instance, the BirA method has been used for controlled protein multimerization,¹⁰ targeting of magnetic resonance imaging probes *in vivo*,¹¹ and modulation of gene expression in yeast.¹² A second labeling system could be useful in similar ways, particularly if it lacks cross-reactivity with endogenous intracellular molecules, in contrast to streptavidin.

Our lab has developed a protein labeling platform using the enzyme lipoic acid ligase (LplA) from *E. coli*. LplA is structurally homologous to BirA, but catalyzes the ligation of lipoic acid, instead of biotin, to an engineered 13-amino acid sequence called the ligase acceptor peptide (LAP), using ATP as an energy source.^{13,14} We have shown that mutagenesis of the substrate binding pocket allows LplA to ligate a variety of unnatural small molecules, including alkyl azides¹⁵ and coumarin fluorophores.^{16,17} QDs, at 10–20 nm in diameter, are far too large to be bound by the enclosed substrate binding pocket of LplA, but we envisioned a two-step targeting scheme analogous to the BirA system. Bioorthogonal chemistries such as the copper-catalyzed azide-alkyne cycloaddition¹⁸ and the strain-promoted Diels-Alder cycloaddition^{19,20} could potentially be used to link QD to protein, but these ($< 10^4 \text{ M}^{-1} \text{ s}^{-1}$ second-order rate constant) are slower than the haloalkane-dehalogenase ligand-receptor pair marketed as “HaloTag”.²¹ Like biotin-streptavidin, the haloalkane-HaloTag interaction is highly specific and has a fast on-rate of $\sim 10^6 \text{ M}^{-1} \text{ s}^{-1}$, which could boost labeling sensitivity.²¹ Once complexed, a nucleophilic substitution reaction between Asp106 of HaloTag and the haloalkane (Figure 1) renders the interaction covalent and irreversible, a desirable feature for our application. Therefore, we decided to explore a QD targeting scheme based on LplA-catalyzed ligation of a haloalkane to LAP, followed by derivatization with HaloTag-conjugated QDs, as shown in Figure 1.

RESULTS AND DISCUSSION

The requirement for a single small molecule to be recognized by both LplA (for ligation to the LAP peptide) and HaloTag (to allow QD targeting) presented an engineering challenge. On the one hand, LplA prefers relatively short substrates measuring less than 9 Å in length.²² On the other hand, HaloTag requires at least 12 Å between the halide and the LAP peptide because the halide-displacing residue, Asp106, is deeply buried within a narrow substrate binding tunnel.²³ Taken together, we expected LplA to set an upper bound on substrate length, and HaloTag to set a lower bound.

Based on these considerations, we screened a panel of six candidate haloalkane substrates using an HPLC assay (Figure 2A). We observed minimal incorporation of the longer 10- or 11-carbon substrates by wild-type LplA, but mutations at Trp37 to smaller amino acids Gly, Ala, and Ser lengthened the substrate binding pocket and facilitated binding of longer substrates (Figure 2A). Overall, the LplA variants did not significantly discriminate chloroalkanes from bromoalkanes of the same chain length.

Having opened the door to longer haloalkanes, we used a cell-based assay to test their reactivity toward HaloTag after ligation to E2p, a 9 kDa lipoyl acceptor domain from *E. coli*.²² Human embryonic kidney 293T (HEK) cells expressing an E2p fusion to a membrane-anchored cyan fluorescent protein (E2p-CFP-TM) were treated with LplA/

haloalkane pairs that had shown appreciable ligase activity *in vitro*, then stained with a HaloTag-Alexa Fluor 568 conjugate (HaloTag-AF568). We compared AF568 over CFP fluorescence ratios by imaging, as a measure of expression level-independent HaloTag labeling (Figure 2B), and found that bromoalkane probes were generally more efficient than chloroalkane probes. Interestingly, although W37A LplA alone preferred the longer 11-bromoundecanoic acid, 10-bromodecanoic acid (10-Br) produced the highest HaloTag staining intensity (Figure 2B). We reasoned that HaloTag may favor the 10-Br-E2p adduct over the 11-Br-E2p adduct because the haloalkane chain of the former may be more extended in aqueous solution. These results allowed us to select 10-Br as the optimal small molecule substrate for two-step labeling, and W37A LplA as its best ligase.

We next characterized the specificity and kinetics of 10-Br ligation onto LAP catalyzed by LplA. For this assay and all subsequent experiments, we used the adenylate ester of 10-bromodecanoic acid (10-Br-AMP, structure and preparation in Supporting Methods) to avoid the use of ATP, which can activate cellular purinergic receptors and cause toxicity.²⁴ We observed W37A LplA-dependent ligation of 10-Br-AMP onto LAP (Supporting Figure 1A), and confirmed the adduct by mass spectrometry (Supporting Figure 1B). We measured the ligation kinetics and obtained a k_{cat} value of $0.020 \pm 0.002 \text{ s}^{-1}$ (Supporting Figure 1C), which is similar to the k_{cat} of our LplA-derived coumarin fluorophore ligase,¹⁶ but is slower than lipoic acid ligation by wild-type LplA ($0.22 \pm 0.01 \text{ s}^{-1}$).¹⁴ When HaloTag was covalently complexed to bromoalkylated LAP, we found that the heterodimers were stable for at least 48 hours (Supporting Figure 2), comparing favorably to the ~several-hour half-life of streptavidin-biotin complexes.

For cellular fluorescence labeling, we optimized the protocol such that, using a 5-minute 10-Br-AMP ligation step plus a 5-minute HaloTag detection step, HEK cells expressing LAP-CFP-TM and stained with HaloTag-AF568 attained a > 15:1 signal-to-noise ratio in imaging (data not shown). Using a gel-shift assay, we measured the overall ligation yield for two steps to be approximately 15% under these conditions (Supporting Figure 3A). Furthermore, HaloTag labeling was not toxic to cells, as assessed by mitochondrial activity (Supporting Figure 3B).

To prepare HaloTag-QD conjugates, we made a Ser59→Cys mutant of HaloTag so that this single solvent-exposed thiolate can be cross-linked to commercially available, amine-functionalized QDs using a maleimide/succinimidyl ester bifunctional crosslinker (Experimental Section). We found that HaloTag-QD605 prepared in this way efficiently labeled HEK cells expressing LAP-tagged low density lipoprotein receptor (LDL receptor), and LAP-tagged synaptic adhesion protein neuexin1 β (Supporting Figure 3C). Labeling was site-specific because a Lys→Ala mutation on LAP eliminated QD staining. We also labeled LAP-LDL receptor on the surface of dissociated rat hippocampal neurons (Supporting Figure 3D), showing that our method is specific and non-toxic even for this delicate cell type.

For many biological studies, it is desirable to image two or more proteins at the same time in the same cell, or in neighboring cells. We attempted to combine the LplA/HaloTag and BirA/streptavidin systems for two-color QD targeting because they are highly analogous yet potentially orthogonal. To confirm this, we used an *in vitro* HPLC assay and observed orthogonal ligation of 10-Br-AMP and biotin onto LAP and AP, respectively (Supporting Figure 4B). We then performed two-color QD labeling on a mixed HEK cell population expressing LAP-CFP-TM or AP-YFP-TM, or both. After 10-Br-AMP ligation by W37A LplA and biotin ligation in the secretory pathway by a co-expressed, endoplasmic reticulum-localized BirA (BirA-ER),²⁵ cells were treated with a mixture of HaloTag-QD605 and streptavidin-QD655. We detected QD fluorescence with the expected pattern for a fully

orthogonal system (Supporting Figure 4C). With sparse application of QDs, we imaged the LDL receptor and the epidermal growth factor receptor (EGF receptor) expressed on the same cell, as well as neurexin1 β and its adhesion partner, neuroligin1, expressed on neighboring cells (Figure 3). In this experiment many QDs exhibited blinking, consistent with single molecule detection (Movie 1).

Labeling would be more straightforward if LAP could be bromoalkylated in the secretory pathway by co-expressed LplA, just as AP is biotinylated by ER-localized BirA, but LplA is generally inactive in oxidizing compartments of the cell.¹⁶ In a separate effort to evolve LplA using yeast display selections, our lab identified a quadruple mutant of the ligase (Trp37 \rightarrow Ala/Thr57 \rightarrow Ile/Phe147 \rightarrow Leu/His267 \rightarrow Arg; three additional mutations compared to W37A LplA) which is active in the ER, termed AILR LplA-ER.²⁶ Expressing this ligase in HEK cells, we successfully targeted HaloTag-Alexa Fluor 647 to cell surface LDL receptors without the need to supply purified LplA to the culture media (Supporting Figure 5).

The exceptional brightness of QDs allows tracking of single mobile targets by imaging. This data provides information about the target that cannot be easily extracted from imaging at the ensemble level. It is well established that pre-synaptic neurexin1 β on one neuron interacts in *trans* with its post-synaptic adhesion partner, neuroligin1 on an apposing neuron,²⁷ but the discovery of neurexins at *post*-synaptic terminals suggested that these two proteins in the same cell may also interact in *cis*.²⁸ As a test of this hypothesis, we expressed LAP-neurexin1 β in HeLa cells and measured its diffusion dynamics by single QD tracking with and without the co-expression of AP-tagged neuroligin1 (AP-neuroligin1) in the same cell. Based on a previous study that found an inverse correlation between a transmembrane protein's size and its diffusion coefficient,²⁹ we expected the lateral movement of LAP-neurexin1 β to slow down if neurexin-neuroligin *cis* interactions occurred. We observed no significant change in neurexin1 β diffusion rates with co-expression of neuroligin1 ($p = 0.2768$, Figure 4A; similar results with reverse tagging orientation shown in Figure 4B), consistent with an absence of *cis*-interactions in HeLa.

CONCLUSION

In summary, we have developed a new QD targeting method based on LplA ligation of a haloalkane to LAP fusion proteins, followed by detection with HaloTag-conjugated QDs. This scheme is analogous to our previously reported BirA-based system, and is similarly sensitive and specific, although HaloTag-QD targeting by LplA is covalent. Because the two methods are orthogonal, they can be used in combination for simultaneous imaging of two different proteins, each with single molecule sensitivity. We demonstrated this capability by two-color single molecule imaging of the LDL receptor and the EGF receptor, as well as of neurexin1 β and neuroligin1 in the same sample.

Numerous other methods have been developed for QD targeting to cellular proteins, and the method we present here offers complementary attributes. First, our method is covalent, and so should be better suited for long-term tracking of single proteins than non-covalent methods such as BirA² and polyhistidine tag³⁰ strategies. Second, even though the HaloTag-QD conjugate is large, our proteins are modified by only a small peptide (13-amino acid LAP) prior to arriving at the cell surface. We have observed in numerous cases that a small tag is much less likely than a large tag to disrupt protein trafficking through the secretory pathway and post-translational processing (Supporting Figure 6A). In an extreme example, a 41 kDa tag fused to the *N*-terminus of neurexin abolishes its surface delivery in neurons, rendering QD labeling impossible, whereas a peptide tag did not prohibit surface expression (Supporting Figure 6B). A QD targeting method reported by Rao *et al.* fuses the protein of interest directly to HaloTag,³¹ which, at 35 kDa, is likely to disrupt trafficking to the cell

surface in many cases. Other methods based on cutinase³² or acyl carrier protein³³ also utilize large fusion tags on the protein from the moment of its synthesis.

We envision applications beyond QD targeting for LplA-mediated bromoalkylation of LAP and its subsequent conjugation to HaloTag, similar to how biotin ligase and streptavidin have been harnessed for diverse applications in macromolecular assembly and nanotechnology. The method reported here could potentially be applied to any problem for which site-specific protein-protein conjugation is beneficial, such as preparation of antibody conjugates, or assembly of nanostructures. The key advantages compared to the biotin ligase system are its covalent nature and the lack of cross-reactivity with endogenous intracellular or serum molecules; in contrast, streptavidin binds to endogenous intracellular biotinylated proteins and can be quenched by free biotin in serum.³⁴

EXPERIMENTAL SECTION

HPLC and ESI mass spectrometric analysis of LplA-catalyzed probe ligation

Peptides treated with lipoic acid ligase (LplA) and small molecule substrate were resolved on a 250 mm × 4.6 mm C₁₈ column with an H₂O/acetonitrile/0.1% trifluoroacetic acid gradient (25% to 60% acetonitrile over 14 min.) using a Varian ProStar HPLC system. Traces show absorbance detection at 210 nm. Peaks of interest were analyzed by ESI (+) mass spectrometry on an Applied Biosystems 200 QTRAP Mass Spectrometer.

Chemical conjugation of HaloTag to QD605

30 μl of 8 μM Qdot 605 ITK amino PEG (Life Technologies) was exchanged into phosphate buffered saline (PBS, pH 7.4) by adding 200 μl PBS and concentrating to 60 μl using a Nanosep 100K Omega ultrafiltration device (PALL) spun at 6000 g at 4 °C. The QDs were then reacted with 7 μl of 10 mM sulfosuccinimidyl 4-*N*-maleimidomethyl]cyclohexane-1-carboxylate (sulfo-SMCC, Pierce) in a 1.5 ml microfuge tube for 1 hour at room temperature on a rotator. Meanwhile, 300 μl of 60 μM ⁵⁵C-HaloTag in PBS (containing 1 mM dithiothreitol, DTT) was run through a NAP-5 column (GE Healthcare) to remove DTT. At the end of the hour, QD605 mixture was purified on a NAP-5 column to remove unreacted sulfo-SMCC. Sulfo-SMCC-derivatized QDs were collected into a 1.5 ml microfuge tube containing the ⁵⁵C-HaloTag protein (total reaction volume ~ 1 ml) and left to react for 1 hour at room temperature on the rotator. Next, 10 μl of 10 mM 2-mercaptoethanol was added to the reaction and left for an additional 30 minutes. to cap unreacted maleimides. Afterwards, the reaction mixture was concentrated to ~ 50 μl using the Nanosep ultrafiltration device. The concentrated mixture was run through a home-packed Sephadex G100 (Sigma) column (12 cm × 0.8 cm I.D.) developed in PBS to remove unconjugated ⁵⁵C-HaloTag and 2-mercaptoethanol. Finally, the eluate was concentrated to ~50 μl as above and then spun at 13000 g in a microfuge tube for 5 minutes at 4 °C to remove aggregated QDs.

Mammalian cell culture and transfection

Unless otherwise stated, human embryonic kidney 293T (HEK), HeLa, or CHO cells were cultured as a monolayer on glass cover slips in complete growth medium: Dulbecco's modified Eagle medium (DMEM, Gibco) supplemented with 10% fetal bovine serum (PAA Laboratories) at 37°C and under 5% CO₂. Adherence of HEK cells was promoted by pre-coating the glass with 50 μg/ml fibronectin (Millipore). Cells were typically transfected at ~70% confluence using Lipofectamine 2000 (Life Technologies) according to the manufacturer's instructions.

Live cell labeling with 10-Br-AMP and staining with HaloTag-conjugated fluorophores

Cells were generally labeled 18–24 hours after transfection. Unless otherwise stated, cells were first treated with fresh growth medium supplemented with 10 μM ^{37}A LpIA, 50 μM 10-Br-AMP, and 5 mM $\text{Mg}(\text{OAc})_2$ for 5 minutes at room temperature (to minimize internalization). After three rinses with the same media, cells were treated with HaloTag-conjugated fluorophores in growth medium for another 5 minutes at room temperature and imaged after three final rinses with Dulbecco's phosphate buffered saline (DPBS, Gibco).

Fluorescence microscopy

For epifluorescence imaging, labeled cells in DPBS were imaged on a Zeiss AxioObserver.Z1 inverted epifluorescence microscope using a 40 \times oil-immersion lens, a CCD camera (Roper Scientific) and the following filter sets: CFP (420/20 ex; 475/40 em; 450 dichroic), YFP (493/16 ex; 525/30 em; 502 dichroic), AF568 (570/20 ex; 605/30 em; 585 dichroic), AF647 (630/10 ex; 685/40 em; 645 dichroic), QD605 (400/120 ex; 605/30 em; 502 dichroic), and QD655 (400/120 ex; 655/20 em; 502 dichroic). Images were acquired and processed using Slidebook version 4.0 (Intelligent Imaging Innovations).

For objective-type total internal reflection fluorescence (TIRF) microscopy, cells were cultured on No. 1.5 glass cover slips and imaged in DPBS on a Zeiss AxioObserver.Z1 inverted microscope (equipped with a Zeiss TIRF slider) using an 100 \times /NA1.46 oil-immersion lens. QDs were excited with a 491 nm diode pumped solid state laser and detected through QD emission filters listed above. Images were processed using Slidebook software version 4.0 (Intelligent Imaging Innovations).

Comparison of haloalkane ligation efficiencies by LpIA variants (Figure 2A)

100 μM E2p protein was mixed with 1 μM LpIA (wild-type or mutant), 5 mM $\text{Mg}(\text{OAc})_2$, 1 mM ATP, and 500 μM haloalkane and reacted at 21 $^\circ\text{C}$ for 1 hour. Reactions were then quenched with 50 mM EDTA (final concentration) and analyzed by Waters Acquity UPLC on a C_{18} column with an H_2O /acetonitrile/0.1% trifluoroacetic acid gradient. Product formation was quantified by comparing peak areas. For simplicity, areas of E2p and E2p adduct peaks (210 nm absorbance detection) were directly used to calculate conversion percentage without accounting for differences in extinction coefficient. All ligated E2p adduct peaks were confirmed by tandem ESI (+) mass spectrometry (data not shown). Negative controls with enzymes omitted showed no E2p conversion (data not shown).

Comparison of HaloTag-AF568 cell surface labeling extents with different LpIA/haloalkane combinations (Figure 2B)

HEK cells were transfected with E2p-CFP-TM and labeled as described above ("Live cell labeling with 10-Br-AMP and staining with HaloTag-conjugated fluorophores") with 1.2 μM HaloTag-AF568 for 5 minutes at 21 $^\circ\text{C}$. 30 cells across 2 fields-of-view from each haloalkane/ligase combination were analyzed in Slidebook for AF568 over CFP fluorescence intensities. Averaged whole-cell AF568 and CFP fluorescence intensities were used, after background subtraction.

Sparse, orthogonal QD targeting to LAP and AP tagged cell surface proteins (Figure 3)

For orthogonal labeling of neurexin1 β and neuroligin1, HeLa cells were either singly transfected with LAP-neurexin1 β , or co-transfected with AP-neuroligin1 and BirA-ER (2:1 plasmid ratio). Cells were then cultured for 20 hours in complete growth medium supplemented with 10 μM biotin (gift from Tanabe USA). Afterwards, HeLa cells were lifted with 0.05% trypsin + 0.53 mM EDTA (Mediatech), mixed, then replated in growth medium containing 10 μM biotin and cultured for another 24 hours. Cells were then rinsed

three times with DPBS followed by treatment with 10 μM W37A Lp1A, 50 μM 10-Br-AMP and 5 mM $\text{Mg}(\text{OAc})_2$ in DMEM containing 1% (w/v) debiotinylated (by extensive dialysis) bovine serum albumin for 5 minutes at room temperature. Sparse QD labeling was achieved by further treatment with a mixture of 10 nM HaloTag-QD605 and 1 nM streptavidin-QD655 (Life Technologies) in the same media for 3 minutes at 21°C. Cells were rinsed 4 times with DPBS before imaging by TIRF microscopy.

For orthogonal labeling of the LDL and EGF receptors, HeLa cells were co-transfected with LAP-LDLR, AP-EGFR,²² and BirA-ER, cultured in growth medium supplemented with 10 μM biotin for 24 hours, then subsequently labeled as described above.

Measurement of neurexin1 β diffusion rates by single-molecule tracking (Figure 4)

For HaloTag-QD targeting to neurexin1 β , HeLa cells were transfected with LAP-neurexin1 β , BirA-ER, and a CFP transfection marker with or without AP-neurologin1 and kept in growth medium supplemented with 10 μM biotin. 18 hours after transfection, cells were treated with 10 μM W37A Lp1A and 50 μM 10-Br-AMP in Tyrode's buffer (145 mM NaCl, 1.25 mM CaCl_2 , 3 mM KCl, 1.25 mM MgCl_2 , 0.5 mM NaH_2PO_4 , 10 mM glucose, 10 mM HEPES, pH 7.4) for 2 minutes at room temperature. Cells were then rinsed with Tyrode's buffer followed by incubation with 10 nM HaloTag-QD605 for 1 minute at room temperature. Upon further rounds of rinsing, the culture dish containing QD-labeled cells was mounted onto a Zeiss Axio Observer.Z1 epifluorescence microscope encased in a 37°C incubating chamber (Okolab). After media change to pre-warmed Tyrode's buffer at 37°C, QD fluorescence from CFP-positive cells was imaged by TIRF microscopy using a 100X objective and recorded at 20 Hz. Single QD tracks were identified and analyzed with Slidebook software. Tracks lasting fewer than 10 frames were discarded. Diffusion coefficients were calculated from the mean square displacement in the first 5 frames, fitted to the equation $\langle(x(t)-x_0)^2\rangle = 4Dt$. Each histogram was constructed from 110–120 QD tracks from 4 cells.

For streptavidin-QD targeting to neurexin1 β , HeLa cells were transfected with AP-neurexin1 β , BirA-ER, and a CFP transfection marker with or without LAP-neurologin1 and similarly kept in biotin-supplemented growth medium. QD targeting was achieved by a 1-minute incubation of 1 nM streptavidin-QD655 in Tyrode's buffer at room temperature. QD fluorescence was recorded after temperature jump (to 37°C) by buffer exchange.

To confirm co-expression of neurologin1 in either experiment, imaged culture dishes were subjected to a second round of QD labeling then re-imaged. Samples for Figure 4A were treated with 10 nM streptavidin-QD655 in Tyrode's buffer for 5 minutes at room temperature. Samples for Figure 4B were enzymatically bromoalkylated as above, then treated with 10 nM HaloTag-QD605 in Tyrode's buffer for 5 minutes at room temperature. Epifluorescence images were acquired at 21°C and showed neurologin1 expression in > 90% CFP-positive cells from samples transfected with neurologin1 (data not shown).

Supplementary Material

Refer to Web version on PubMed Central for supplementary material.

Acknowledgments

We thank the NIH (R01 GM072670), MIT, and the Dreyfus Foundation for funding. M. Howarth was supported by a Computational and Systems Biology Initiative MIT-Merck postdoctoral fellowship. G. Los (Promega) provided the HaloTag gene. M. Yamagata (Harvard) provided the neurexin and neurologin genes. P. Zou (MIT) provided technical assistance and the LDL receptor gene. S. Johnston and M. Lewandowski (Broad Institute) provided assistance with UPLC. K. White (UCSF) provided the AILR Lp1A-ER plasmid.

References

1. Pinaud F, Clarke S, Sittner A, Dahan M. Probing Cellular Events, One Quantum Dot at a Time. *Nat Methods*. 2010; 7:275–285. [PubMed: 20354518]
2. Howarth M, Takao K, Hayashi Y, Ting AY. Targeting Quantum Dots to Surface Proteins in Living Cells with Biotin Ligase. *Proc Natl Acad Sci U S A*. 2005; 102:7583–7588. [PubMed: 15897449]
3. Bates IR, Hebert B, Luo Y, Liao J, Bachir AI, Kolin DL, Wiseman PW, Hanrahan JW. Membrane Lateral Diffusion and Capture of CFTR within Transient Confinement Zones. *Biophys J*. 2006; 91:1046–1058. [PubMed: 16714353]
4. Sung K, Maloney MT, Yang J, Wu C. A Novel Method for Producing Mono-Biotinylated, Biologically Active Neurotrophic Factors: An Essential Reagent for Single Molecule Study of Axonal Transport. *J Neurosci Methods*. 2001; 200:121–128. [PubMed: 21756937]
5. Howarth M, Liu W, Puthenveetil S, Zheng Y, Marshall LF, Schmidt MM, Wittrup KD, Bawendi MG, Ting AY. Monovalent, Reduced-Size Quantum Dots for Imaging Receptors on Living Cells. *Nat Methods*. 2008; 5:397–399. [PubMed: 18425138]
6. Swift JL, Cramb DT. Nanoparticles as Fluorescence Labels: Is Size All that Matters? *Biophysical Journal*. 2008; 95:865–876. [PubMed: 18390610]
7. Bruneau E, Sutter D, Hume RI, Akaaboune M. Identification of Nicotinic Acetylcholine Receptor Recycling and Its Role in Maintaining Receptor Density at the Neuromuscular Junction. *In Vivo J Neurosci*. 2005; 25:9949–9959.
8. Pierres A, Touchard D, Benoliel A-M, Bongrand P. Dissecting Streptavidin-Biotin Interaction with a Laminar Flow Chamber. *Biophys J*. 2002; 82:3214–3223. [PubMed: 12023246]
9. Chivers CE, Crozat E, Chu C, Moy VT, Sherratt DJ, Howarth M. A Streptavidin Variant with Slower Biotin Dissociation and Increased Mechanostability. *Nat Methods*. 2010; 7:391–393. [PubMed: 20383133]
10. Yang J, Jaramillo A, Shi R, Kwok WW, Mohanakumar T. *In Vivo* Biotinylation of the Major Histocompatibility Complex (MHC) Class II/Peptide Complex by Coexpression of BirA Enzyme for the Generation of MHC Class II/Tetramers. *Hum Immunol*. 2004; 65:692–699. [PubMed: 15301857]
11. Tannous BA, Grimm J, Perry KF, Chen JW, Weissleder R, Breakefield XO. Metabolic Biotinylation of Cell Surface Receptors for *In Vivo* Imaging. *Nat Methods*. 2006; 3:391–396. [PubMed: 16628210]
12. Athavankar S, Peterson BR. Control of Gene Expression with Small Molecules: Biotin-Mediated Acylation of Targeted Lysine Residues in Recombinant Yeast. *Chem Biol*. 2003; 10:1245–1253. [PubMed: 14700632]
13. Green DE, Morris TW, Green J, Cronan JE, Guest JR. Purification and Properties of the Lipoate Protein Ligase of *Escherichia coli*. *Biochem J*. 1995; 309:853–862. [PubMed: 7639702]
14. Puthenveetil S, Liu DS, White KA, Thompson S, Ting AY. Yeast Display Evolution of a Kinetically Efficient 13-Amino Acid Substrate for Lipoic Acid Ligase. *J Am Chem Soc*. 2009; 131:16430–16438. [PubMed: 19863063]
15. Yao JZ, Uttamapinant C, Poloukhine A, Baskin JM, Codelli JA, Sletten EM, Bertozzi CR, Popik VV, Ting AY. Fluorophore Targeting to Cellular Proteins *via* Enzyme-Mediated Azide Ligation and Strain-Promoted Cycloaddition. *J Am Chem Soc*. 2012; 134:3720–3728. [PubMed: 22239252]
16. Uttamapinant C, White KA, Baruah H, Thompson S, Fernandez-Suarez M, Puthenveetil S, Ting AY. A Fluorophore Ligase for Site-Specific Protein Labeling Inside Living Cells. *Proc Natl Acad Sci U S A*. 2010; 107:10914–10919. [PubMed: 20534555]
17. Cohen JD, Thompson S, Ting AY. Structure-Guided Engineering of a Pacific Blue Fluorophore Ligase for Specific Protein Imaging in Living Cells. *Biochemistry*. 2011; 50:8221–8225. [PubMed: 21859157]
18. Hong V, Steinmetz NF, Manchester M, Finn MG. Labeling Live Cells by Copper-Catalyzed Alkyne-Azide Click Chemistry. *Bioconjug Chem*. 2010; 21:1912–1916. [PubMed: 20886827]
19. Han H-S, Devaraj NK, Lee J, Hilderbrand SA, Weissleder R, Bawendi MG. Development of a Bioorthogonal and Highly Efficient Conjugation Method for Quantum Dots Using Tetrazine-Norbornene Cycloaddition. *J Am Chem Soc*. 2010; 132:7838–7839. [PubMed: 20481508]

20. Liu DS, Tangpeerachaikul A, Selvaraj R, Taylor MT, Fox JM, Ting AY. Diels-Alder Cycloaddition for Fluorophore Targeting to Specific Proteins Inside Living Cells. *J Am Chem Soc.* 2012; 134:792–795. [PubMed: 22176354]
21. Los GV, Encell LP, McDougall MG, Hartzell DD, Karassina N, Zimprich C, Wood MG, Learish R, Ohana RF, Urh M, et al. HaloTag: A Novel Protein Labeling Technology for Cell Imaging and Protein Analysis. *ACS Chem Biol.* 2008; 3:373–382. [PubMed: 18533659]
22. Fernández-Suárez M, Baruah H, Martínez-Hernández L, Xie KT, Baskin JM, Bertozzi CR, Ting AY. Redirecting Lipoic Acid Ligase for Cell Surface Protein Labeling with Small-Molecule Probes. *Nat Biotechnol.* 2007; 25:1483–1487. [PubMed: 18059260]
23. Newman J, Peat TS, Richard R, Kan L, Swanson PE, Affholter JA, Holmes IH, Schindler JF, Unkefer CJ, Terwilliger TC. Haloalkane Dehalogenases: Structure of a *Rhodococcus* Enzyme. *Biochemistry.* 1999; 38:16105–16114. [PubMed: 10587433]
24. Rathbone MP, Middlemiss PJ, Gysbers JW, Andrew C, Herman MA, Reed JK, Ciccarelli R, Di Iorio P, Caciagli F. Trophic Effects of Purines in Neurons and Glial Cells. *Prog Neurobiol.* 1999; 59:663–690. [PubMed: 10845757]
25. Howarth M, Ting AY. Imaging Proteins in Live Mammalian Cells with Biotin Ligase and Monovalent Streptavidin. *Nat Protoc.* 2008; 3:534–545. [PubMed: 18323822]
26. White, KA. Thesis. Massachusetts Institute of Technology; 2012. Rational Design and Directed Evolution of Probe Ligases for Site-Specific Protein Labeling and Live-Cell Imaging.
27. Craig AM, Kang Y. Neurexin-Neuroigin Signaling in Synapse Development. *Curr Opin Neurobiol.* 2007; 17:43–52. [PubMed: 17275284]
28. Taniguchi H, Gollan L, Scholl FG, Mahadomrongkul V, Dobler E, Limthong N, Peck M, Aoki C, Scheiffele P. Silencing of Neuroigin Function by Postsynaptic Neurexins. *J Neurosci.* 2007; 27:2815–2824. [PubMed: 17360903]
29. Thoumine O, Saint-Michel E, Dequidt C, Falk J, Rudge R, Galli T, Faivre-Sarraillh C, Choquet D. Weak Effect of Membrane Diffusion on the Rate of Receptor Accumulation at Adhesive Contacts. *Biophys J.* 2005; 89:40–42.
30. Roullier V, Clark S, You C, Pinaud F, Gouzer GG, Schaible D, Marchi-Artzner V, Piehler J, Dahan M. High-Affinity Labeling and Tracking of Individual Histidine-Tagged Proteins in Live Cells Using Ni²⁺ Tris-Nitrilotriacetic Acid Quantum Dot Conjugates. *Nano Lett.* 2009; 9:1228–1234. [PubMed: 19216518]
31. So M, Yao H, Rao J. HaloTag Protein-Mediated Specific Labeling of Living Cells with Quantum Dots. *Biochem Biophys Res Commun.* 2008; 374:419–423. [PubMed: 18621022]
32. Bonasio R, Carman CV, Kim E, Sage PT, Love KR, Mempel TR, Springer TA, von Andrian UH. Specific and Covalent Labeling of a Membrane Protein with Organic Fluorochromes and Quantum Dots. *Proc Natl Acad Sci U S A.* 2007; 104:14753–14758. [PubMed: 17785425]
33. George N, Pick H, Vogel H, Johnsson N, Johnsson K. Specific Labeling of Cell Surface Proteins with Chemically Diverse Compounds. *J Am Chem Soc.* 2004; 126:8896–8897. [PubMed: 15264811]
34. Atamna H, Newberry J, Erlitzki R, Schultz CS, Ames BN. Biotin Deficiency Inhibits Heme Synthesis and Impairs Mitochondria in Human Lung Fibroblasts. *J Nutr.* 2007; 137:25–30. [PubMed: 17182796]

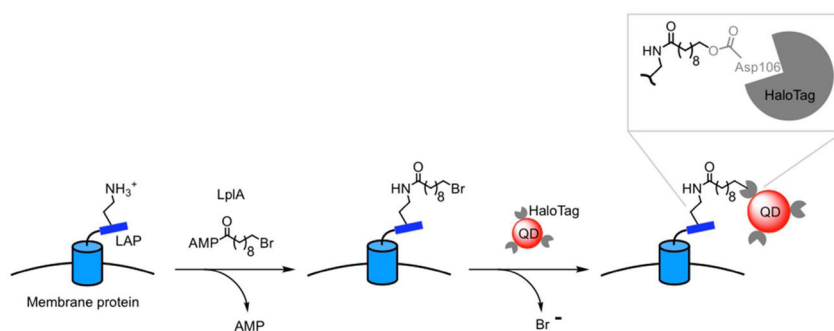


Figure 1. Scheme for lipoic acid ligase (LplA)- and HaloTag-mediated two-step quantum dot (QD) targeting to membrane proteins. In the first step, LplA site-specifically ligates 10-bromodecanoic acid adenylate ester (10-Br-AMP, complete structure in Supporting Information) onto the lysine side chain of ligase acceptor peptide (LAP). In the second step, HaloTag-conjugated QDs covalently react with bromoalkylated proteins. **Inset:** in the final complex, Asp106 of HaloTag is covalently linked to the LAP tag *via* an ester bond.

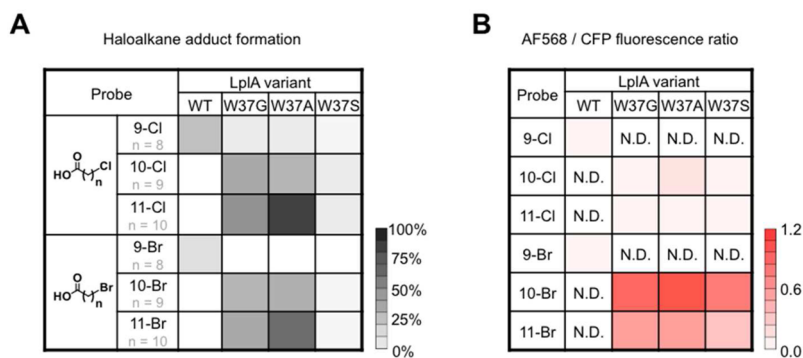


Figure 2. Comparison of LplA variants for *in vitro* haloalkane ligation and cell surface HaloTag targeting. **(A)** Purified E2p protein was treated with one of six haloalkane substrates and one of four LplA variants – wild-type (WT) or a Trp37 → Gly/Ala/Ser mutant. After one hour, E2p-haloalkane adduct formation was quantified by HPLC. Gray-scale indicates the percentage conversion to product. **(B)** HEK cells expressing E2p-CFP-TM were treated with the LplA and haloalkane pairs for 5 min., then stained with HaloTag-AF568 for 5 min. and imaged. AF568 over CFP fluorescence ratios were calculated from 30 cells for each condition, and the averages are indicated with red-scale. “N. D.” denotes “not determined”, for conditions giving low efficiency in (A).

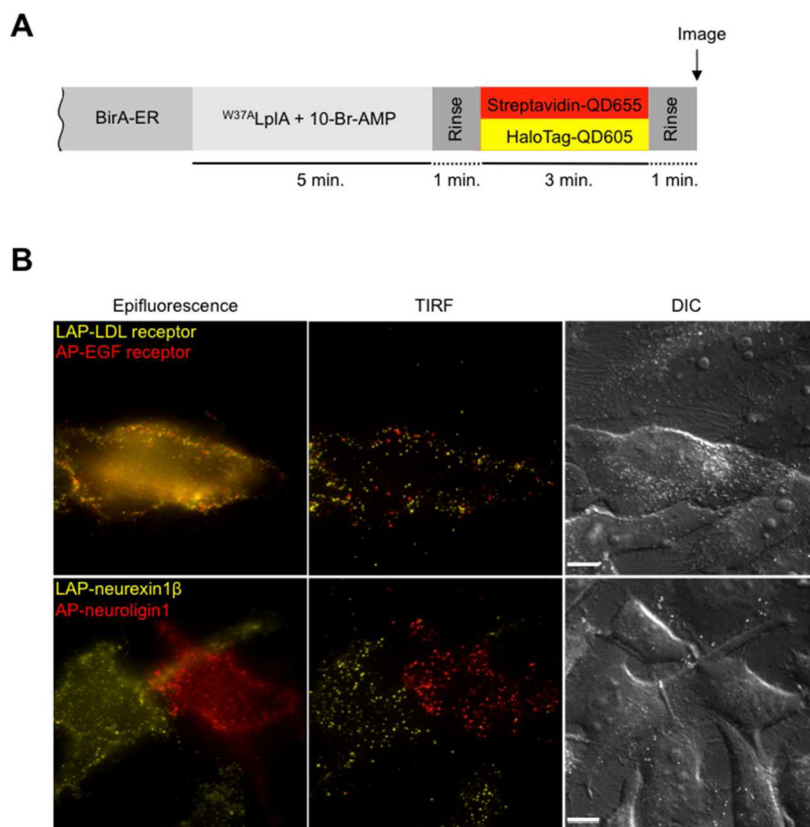


Figure 3. Orthogonal QD targeting to LAP and BirA acceptor peptide (AP) fusion proteins for two-color single molecule imaging. **(A)** Labeling protocol. Biotinylation of AP was achieved in the secretory pathway by an endoplasmic reticulum-localized BirA (BirA-ER). 10-Br-AMP ligation onto LAP was catalyzed by purified W^{37A} LpIA added to the culture media. After rinsing, cells were simultaneously treated with HaloTag-QD605 and streptavidin-QD655. **(B)** HeLa cultures expressing LAP-LDL receptor and AP-EGF receptor on the same cell (top row), or LAP-neurexin1 β and AP-neuroigin1 on neighboring cells (bottom row) were labeled according to the scheme in (A) with 1–10 nM QDs and imaged live. QD605 (yellow) and QD655 (red) were imaged under epifluorescence and total internal reflection fluorescence (TIRF) modes and shown next to DIC images. Scale bars, 10 μ m. Movie 1 shows time-lapse TIRF imaging of LAP-neurexin1 β and AP-neuroigin1, labeled as in (B).

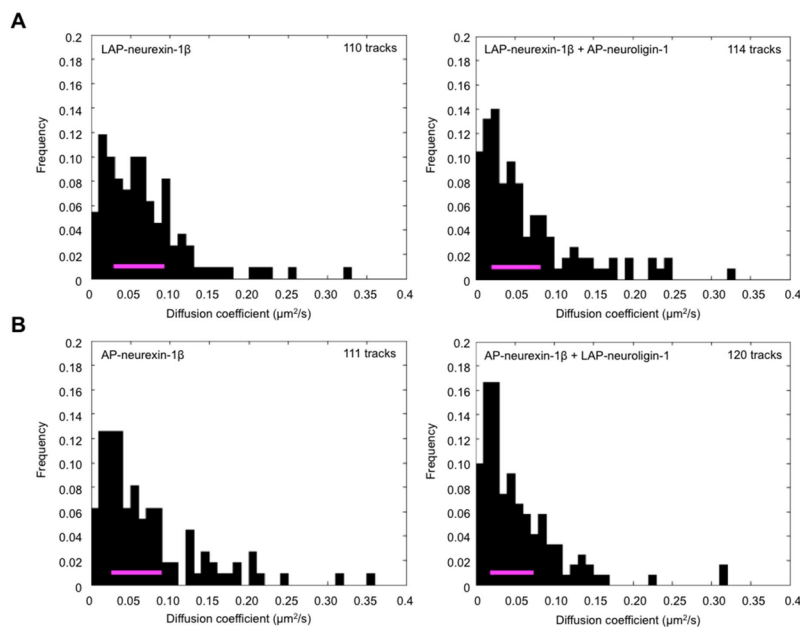


Figure 4.

Measurement of neurexin1 β diffusion in the presence vs. absence of neuroligin1 by single-molecule tracking. **(A) Left:** HeLa cells expressing LAP-neurexin1 β were labeled with HaloTag-QD605, then imaged live by TIRF microscopy at 20 Hz. Individual QD tracks from 4 cells were used to calculate diffusion coefficients, plotted here as a histogram. **Right:** The same experiment, but with AP-neuroligin1 co-expressed. Diffusion coefficients were not significantly different ($p = 0.2768$). **(B)** The same experiment as in (A), but with the labels reversed. Neurexin1 β was tagged with AP and labeled with streptavidin-QD655. On the right, LAP-neuroligin1 was co-expressed. Again, the diffusion coefficients were not significantly changed by co-expression of neuroligin1 ($p = 0.3165$). Pink bars indicate interquartile ranges.